INCREASED VASCULARITY AND SPONTANEOUS METASTASIS OF BREAST CANCER BY HEDGEHOG SIGNALING MEDIATED UPREGULATION OF CYR61

Lillianne G. Harris, **Lewis K. Pannell**, **Seema Singh**, **Rajeev S. Samant**, and **Lalita A. Shevde**[*]

Department of Oncologic Sciences, Mitchell Cancer Institute, University of South Alabama, Mobile, AL

Abstract

The Hedgehog (Hh) pathway is well known for its involvement in angiogenesis and vasculogenesis during ontogeny. The ligand, Sonic hedgehog (SHH), plays an important role in vascular formation during development. However, SHH expression is upregulated on tumor cells and can impact the tumor microenvironment. We have investigated the effects of autocrine as well as paracrine Hh signaling on tumor cells as well as on endothelial cells, respectively.

Upon constitutive expression of SHH, breast cancer cells showed aggressive behavior and rapid xenograft growth characterized by highly angiogenic tumors that were spontaneously metastatic. In these cells, SHH caused activation of the Hh transcription factor, GLI1, leading to upregulated expression of the potent pro-angiogenic secreted molecule, CYR61 (cysteine rich angiogenic inducer 61). Silencing of CYR61 from these SHH-expressing Hh activated cells blunted the malignant behavior of the tumor cells and resulted in reduced tumor vasculature and limited hematogenous metastases. Thus, CYR61 is a critical downstream contributor to the Hh influenced pro-angiogenic tumor microenvironment. We also observed concomitant upregulation of SHH and CYR61 transcripts in tumors from patients with advanced breast cancer, further ratifying the clinical relevance of our findings. In summary, we have defined a novel, VEGF-independent, clinically relevant, pro-angiogenic factor, CYR61, that is a transcriptional target of Hh-GLI signaling.

Keywords

SHH; CYR61; GLI; Hedgehog; angiogenesis; metastasis

[*]To whom correspondence should be addressed at: Lalita A. Shevde, MCI 3018, USA-Mitchell Cancer Institute, 1660 Springhill Avenue, Mobile, AL 36604. lsamant@usouthal.edu; Tel: 251-445-9854 .

CONFLICT OF INTEREST

The authors declare no conflict of interest.

Hedgehog pathway upregulates CYR61

INTRODUCTION

While anti-vascular therapies have been useful in shrinking tumors and in increasing the time-to-progression (Fox *et al.*, 2007; Samant and Shevde, 2011), to date, very few of these drugs have been effective in promoting long term survival (Fox *et al.*, 2007). Redundancy in pathways and growth factors that support the formation of tumor neo-vasculature contribute to rapid vascular re-growth in tumors after discontinuation of anti-angiogenic treatment (Mancuso *et al.*, 2006). Thus, there is a need for alternate targets and strategies to treat tumor vasculature to combat intrinsic resistance and acquired resistance to anti-angiogenic drugs.

The Hedgehog (Hh) pathway is activated in several cancers (Merchant and Matsui, 2010; Yang *et al.*, 2010). Canonical Hh pathway activation ensues the binding of ligands, SHH/IHH/DHH to the extracellular domain of the membrane bound receptor Patched (PTCH) (Beachy *et al.*, 2010). This causes a release of inhibitory actions of PTCH on Smoothed, SMO (Reviewed by (Cohen, 2010)) which results in the activation of the GLI family of transcription factors. The Hh pathway has been studied for its involvement in angiogenesis and vasculogenesis during ontogeny (Hochman *et al.*, 2006). In cancer, aberrant upregulation of Hh signaling impacts the tumor microenvironment and contributes to tumor progression (Bailey *et al.*, 2009; Cao *et al.*, 2011; O'Toole *et al.*, 2011; Zunich *et al.*, 2009).

In this study we report the identification of a novel, VEGF-independent, clinically relevant, transcriptional target of Hh-GLI signaling, CYR61 (cysteine rich angiogenic inducer 61). We have investigated the impact of autocrine/homotypic Hh signaling on tumor cells and have also characterized paracrine Hh signaling involving tumor cells and endothelial cells. Hh signaling mediated upregulation of CYR61 in breast cancer cells causes an increase in tumor vasculature and supports an environment for metastasis. Thus, strategies targeting Hh signaling could potentially form an effective approach for intervening in tumor vascularization.

RESULTS

Expression of SHH in breast cancer cells enhances their malignant attributes

In order to assess the role of Hh signaling in breast tumor vascularity and metastasis, we engineered breast cancer cell lines with endogenously low expression of the prominent Hh pathway activating molecule, SHH, to constitutively express this ligand. Human breast cancer cells, MDA-MB-231 and MCF10AT were selected not only for their relatively low expression of SHH but also due to the fact that both cell lines are incapable of spontaneous metastasis in xenograft models of breast cancer (Santner *et al.*, 2001; Zhang *et al.*, 1991). We detected the 19 kDa fragment which is classically secreted and is the biologically active fragment in conditioned media (Porter *et al.*, 1995) (Figure 1A, Supplementary Figure 1A).

Expression of SHH caused activation of Hh signaling in the cells as indicated by the increase in GLI reporter activity in SHH expressing cells compared to the vector control group ($p < 0.0001$) (Supplementary Figure 1B) as well as an increase in the transcript levels

of PTCH, also a GLI-target gene (data not shown) (Lu *et al.*, 2008; Mukherjee *et al.*, 2006). We assessed the impact of constitutive Hh signaling on attributes of malignancy including cell proliferation, anchorage and contact independent growth, motility and invasion. SHH expressing cells displayed significantly rapid proliferation (p < 0.0001) with an average doubling time of 27 hrs compared to vector control cells (32 hrs) (Figure 1B). SHH expression also significantly enhanced the ability for contact-independent growth (foci formation assay; p = 0.03) and anchorage-independent growth (soft agar assay; p < 0.0001) (Figures 1C and D). SHH expressing cells displayed significantly enhanced motility (p < 0.0001) (Figures 1E) and invasion through basement membrane (p < 0.0001) (Figure 1F). Similar to the MDA-MB-231-SHH expressing cells, the MCF10AT-SHH expressing transfectants also exhibited significantly increased ability to grow in soft agar and were more motile compared to the vector-transfectants (p < 0.0001) (Supplementary Figures 1C & D).

In vivo, SHH-expressing MDA-MB-231 cells showed increased tumor take rate/incidence (Figure 2A). Notably, we used only one-fifth the numbers of cells that are usually used in orthotopic injections in order to assess the impact of constitutive Hh signaling on the tumorigenicity of cells (Shevde *et al.*, 2006). Within 10 days of injection, all the SHH-expressing breast cancer cells had established palpable tumors in contrast to the vector control cells that showed a notable lag in tumor take rate (Figure 2B). SHH expressing breast cancer cell lines also displayed exponential growth compared to the vector control groups (p < 0.0001) (Figure 2B). This may be likely due to the rapid proliferative rates of SHH-expressing cells. The tumors developed from SHH-expressing cells showed prominent, complex blood vessel formations which were larger than the tumors of the vector control group (Figure 2C). Immunohistochemically, the SHH-expressing tumors showed a greater staining intensity (immunoreactive scores) for SHH (p < 0.0001) and significantly greater numbers of proliferating cells as seen by the higher Ki67 labeling index (p < 0.01) and enhanced vascularization (p < 0.005) as evidenced by the increased (doubled relative to control) blood vessel density evident upon staining for Griffonia Simplicifolia Lectin I (Figures 2D & E). Ten weeks post tumor removal the lungs were assessed for evidence of pulmonary metastasis. Notably, 100% of the mice injected with SHH-expressing MDA-MB-231 cells showed pulmonary metastases (Figure 2F). We were also able to recover viable EGFP-expressing tumor cells from the lungs (Figure 2G). These cells expressed SHH at levels that were comparable to the injected cells (data not shown). In the light of the fact that the MDA-MB-231 cells cannot spontaneously metastasize, our data are exciting and implicate a role for Hh signaling in imparting metastatic potential upon tumor cells, likely due to enhancing the malignant potential of the tumor cells *per se* and also by increasing vascularity of the tumor.

Factors secreted by breast cancer cells with constitutive Hh signaling promote pro-angiogenic behavior of endothelial cells in vitro

Increased tumor vascularity suggested a crosstalk between tumor cells and endothelial cells. In order to determine the impact of constitutive Hh signaling in the breast cancer cells on their ability to influence endothelial cells, we assessed the response of endothelial cells to conditioned media from the SHH-expressing breast cancer cells specifically with regard to

migration, ability to invade extracellular matrices and form networks. As depicted in Figures 3A & B, conditioned media from SHH-expressing MDA-MB-231 cells significantly enhanced the ability of endothelial cells of chemotactic migration ($p < 0.005$) and degradation/invasion extracellular matrix proteins ($p < 0.02$). The endothelial cells were also able to efficiently form networks ($p < 0.0001$) (Figure 3C & Supplementary Figure 1E) in the presence of conditioned media from the SHH-expressing cells. The conditioned media from the SHH-expressing cells was more potent ($p < 0.01$) in inducing network formations relative to VEGF, which was used as a positive control. Notably, recombinant SHH was not as efficient at influencing invasive behavior of endothelial cells ($p < 0.005$) and only a high concentration of SHH (50nM) was as potent as the conditioned medium in enhancing migration of the endothelial cells (Figure 3A & Supplementary Figure 2A), implying that additional components in the conditioned medium of the SHH-expressing breast cancer cells may influence endothelial cell behavior.

CYR61 is differentially expressed as a consequence of Hh signaling

In order to identify candidate targets generated via Hh signaling in breast cancer which may contribute to potentiating endothelial cell behavior and vascularization of the tumor xenograft, we used mass spectrometry to analyze and compare the secretomes of SHH-expressing and vector control groups. SHH protein was not detected amongst > 250 proteins detected from the secretome of the vector-control cells. In contrast, SHH was the 33rd most abundant protein (based on Mascot scores) in the secretome from the SHH-expressing MDA-MB-231 cells. Corresponding to this change, we noted that CYR61 had a concomitant increase in abundance with a mascot score of over double that in the vector-transfectant cells. The same increase in abundance was also apparent using spectral counting where the vector-transfectant cells showed only 9 peptide hits, whereas the SHH-expressing MDA-MB-231 cells had 20 hits for CYR61.

In concordance with this data, the SHH-expressing cells show upregulated levels of CYR61, at the transcript levels, as well as in the secretome (immunoblot analysis) (Figure 4A, Supplementary Figure 2B). The xenografts from MDA-MB-231 cells expressing SHH also showed intense staining of CYR61 (Supplementary Figure 2C). Since activated Hh signaling culminates in the nuclear translocation of the GLI transcription factors, we speculated that CYR61 may be a GLI1 target gene. Our search revealed a putative GLI1-binding site within ~1 kb upstream of the CYR61 transcription start site (Figure 4B). The CYR61 promoter is activated ($p < 0.0001$) in SHH-expressing cell lines (Figure 4C, Supplementary Figure 2D). Moreover, mutation or deletion of the GLI1 binding site in the CYR61 promoter significantly abrogated the activity of the CYR61 promoter in the presence of GLI1 (Figure 4D, Supplementary Figure 2E). To further validate the functionality of the GLI1-CYR61 promoter binding relationship, we performed a ChIP analysis. We found that GLI1 binds the CYR61 promoter region as evidenced by a PCR product using GLI1-specific primers. Moreover, the SHH-expressing cell lines yielded a more robust PCR product upon amplification of the immunoprecipitated DNA further confirming that GLI1 transcriptionally enhances CYR61 (Figure 4E).

Hh signaling mediated CYR61 expression contributes to enhanced breast cancer malignancy

CYR61 promotes cell migration, chemotaxis and growth factor-induced DNA synthesis (Feng *et al.*, 2008; Kleer *et al.*, 2007; Sun *et al.*, 2008) and is reported to be pro-angiogenic (Chen *et al.*, 2001; Lin *et al.*, 2005). In order to determine the specific role of CYR61 downstream Hh signaling, we silenced the expression of CYR61 in SHH-expressing MDA-MB-231 cells using shRNA (Figure 5A). This resulted in decreased invasion ($p < 0.0001$) of the tumor cells (Figure 5B) and compromised their ability to induce endothelial cell network formation ($p < 0.0001$) (Figure 5C). While there was no change in the rate of proliferation *in vitro* (data not shown), *in vivo*, CYR61 knockdown resulted in a decrease in tumor growth rates ($p = 0.01$) (Figure 5D) that was characterized by tumors that were notably less vascularized with fewer Ki67-positive cells/nuclei relative to the scrambled control-transfected SHH-expressing tumors (Figure 5E). Also, the SHH-expressing CYR61-silenced xenografts from the MDA-MB-231 cells showed lower immunoreactive scores for CYR61, microvessel density, MVD ($p < 0.001$) and a lower Ki67 labeling index ($p < 0.01$), supporting our finding that silencing CYR61 results in slower-growing tumors, despite continued Hh signaling due to SHH expression (Figure 5F). The expression of SHH was comparable between the 'Scrambled' control (Scram) and cells silenced stably for CYR61. The xenografts developed from cells silenced for CYR61 were also significantly less efficient in colonizing the lungs ($p = 0.01$) (Figure 5G).

SHH and CYR61 expression are concomitantly elevated in advanced breast cancer

We assessed clinical relevance of our findings by querying the expression of transcripts encoding SHH and CYR61 in normal breast tissue as well as breast tumor tissue. The expression of SHH and CYR61 are concomitantly greater in tissues representing advanced stage breast cancer ($p < 0.01$) patients (Figures 6A & B) demonstrating the co-linear expression between SHH and CYR61 and their amplified transcript levels in advanced breast cancer. Notably, the transcript levels of SHH are smaller relative to those of CYR61; smaller changes in the levels of the SHH ligand correlate with transcript levels of a larger magnitude for a transcriptional target such as CYR61.

DISCUSSION

The Hh pathway is activated in several types of cancers and has been implicated in contributing to tumor growth, progression and metastasis (Bailey *et al.*, 2009; Das *et al.*, 2009; Das *et al.*, 2011; Mazumdar *et al.*, 2011; Yang *et al.*, 2010). Angiogenesis is a critical component of tumor metastasis. The vascular density of a tumor has been correlated with metastasis and with patient outcome and can function as an independent prognostic variable in breast cancer (Weidner *et al.*, 1991) (reviewed in (Zetter, 1998)). Our current work has defined a role for Hh signaling in functionally regulating breast cancer malignancy and vascularization. Furthermore, we have identified a novel target of GLI-Hh signaling, CYR61 which appears to be a contributing factor to the enhanced angiogenic and metastatic potential associated with Hh activation in breast cancer.

Hh signaling has been well characterized for its role in embryonic angiogenesis (Byrd and Grabel, 2004; Pola *et al.*, 2001; Vokes *et al.*, 2004) (reviewed in (Bicknell and Harris, 2004)) and in adults during wound healing and in the repair of ischemia (Pola *et al.*, 2001). In tumors, SHH induces the expression of angiopoietins I and II and the family of VEGF-A, B and C from mesenchymal cells, highlighting the significance of Hh signaling in tumor associated fibroblasts to mediate tumor blood vessel formation (Kanda *et al.*, 2003). While much of the anti-angiogenic research has focused on VEGF, the success of anti-angiogenic treatment is limited by low efficacy, mainly due to inadequate alternate targets and strategies that can eliminate resistant cells during treatment-induced tumor regression and due to paucity of selective drugs (Blagosklonny, 2004). The survival of resistant cells is favored by the fact that there is redundancy in the pathways and growth factors that support formation of tumor neo-vasculature. The possible synergistic effects of these growth factors could contribute to rapid vascular re-growth in tumors after discontinuation of anti-angiogenic treatment (Mancuso *et al.*, 2006).

The angiogenic program requires the degradation of the basement membrane, endothelial cell migration, invasion of the extracellular matrix with endothelial cell proliferation and capillary lumen formation before maturation and stabilization of the new vasculature. Our research shows that breast cancer cells with constitutive Hh signaling can enhance the pro-angiogenic behavior of endothelial cells causing the tumor to be vascularized with dichotomous, large-diameter blood vessels. Our observations support previous reports of SHH enhanced vascularization following ischemia (Pola *et al.*, 2001).

Importantly, while secretome analysis did not reveal VEGF among the top 500 proteins, CYR61 was differentially upregulated in the SHH-expressing cells. CYR61 expression, like several of the key molecules in the Hh pathway, is upregulated in clinical evaluation of transformed tissues (Xie *et al.*, 2001b; Xie *et al.*, 2004; Zhou *et al.*, 2009). Furthermore, there appears to be a correlation between the stage of cancer and CYR61 expression in that more advanced cancers often display increased expression of CYR61 (Tsai *et al.*, 2002; Xie *et al.*, 2001a; Xie *et al.*, 2001b). CYR61 has been shown to play a role in decreasing sensitivity to chemotherapeutic drugs such as Taxol (Lai *et al.*, 2011). Conversely, Dobroff and colleagues have reported that CYR61 is a tumor suppressor in melanoma (Dobroff *et al.*, 2009). Since CYR61 and several of the other targets and molecules associated with Hh signaling are secreted, it is important to consider the overall tumor microenvironment, which is often unique for different types of cancers and is specific to individual patients. These differences may dictate the mechanisms of action as well as the overall effects of these molecules. We reported that in melanoma, Hh signaling upregulates osteopontin (OPN) which contributes to increased malignancy of melanoma (Das *et al.*, 2009). Perhaps in some contexts and in very specific niches, Hh signaling selectively modulates the tumor microenvironment. Also, both OPN and CYR61 function through the binding of integrins and HSP, heparin sulfate proteoglycans (Chen and Lau, 2009). Thus the distribution, expression and availability of signaling molecules' receptors may need to be considered in each type of cancer.

O'Toole and others have recently reported an association of Hh signaling with stromal components in breast cancer (O'Toole *et al.*, 2011). In our study, the upregulation of CYR61

as a downstream event of Hh signaling allowed the tumor to be richly vascularized and created permissive conditions for hematogenous metastasis. Further evidence from our lab indicates that the expression of CYR61 is reduced when the expression of GLI1 is abrogated from tumor cells (ongoing work; unpublished data).

It remains unclear as to whether Hh ligands can activate canonical Hh signaling in endothelial cells. However, a growing body of work confirms that Hh ligands can induce pro-angiogenic endothelial behavior such as migration and network formation (Chinchilla *et al.*, 2010; Renault *et al.*, 2010). It is a well accepted fact though, that CYR61 directly induces endothelial cell migration, network formation and tissue remodeling associated with angiogenesis (Babic *et al.*, 1998; Leu *et al.*, 2002). In the present study, we have elucidated the impact of autocrine as well as paracrine Hh signaling on tumor cells as well as endothelial cells, respectively. Such signaling fortifies the tumor microenvironment and supports cross talk between cell types. Taken together, our data suggests that Hh ligands (SHH) may synergize with CYR61 produced by breast cancer cells to induce robust tumor vascularization *in vivo*. Since the concomitant deregulated expression of these molecules supports increased tumor vasculature, it can be speculated that in a clinical context, upregulated expression of SHH and CYR61 in the primary tumor may suggest an increased likelihood of metastasis and thus provide preemptive opportunities for therapeutic intervention.

In sum, we have defined a novel, VEGF-independent, clinically relevant, transcriptional target of Hh signaling, CYR61, that enhances tumor vascularization and promotes spontaneous hematogenous metastasis of breast tumor cells. As such, paracrine Hh signaling and CYR61 present attractive targets to design alternative strategies and mitigate resistance to conventional anti-angiogenic therapy.

MATERIALS & METHODS

Cell Lines and Cell Culture

MDA-MB-231 and COS7 cells were cultured in Dulbeco's Modified Eagle Medium/F12 (Invitrogen, Carlsbad, CA) supplemented with fetal bovine serum (Atlanta Biologicals, Atlanta GA), sodium pyruvate (Invitrogen) and non-essential amino acids (Invitrogen). MCF10AT cells were cultured in DMEM/F12 (Invitrogen) supplemented with horse serum (ATCC, Manassas VA), insulin (Sigma-Aldrich, St.Louis MO), epidermal growth factor (Sigma-Aldrich), cholera toxin (Sigma-Aldrich), and hydrocortisone (Sigma-Aldrich). Cells were grown at 37°C in a humidified 5 % CO_2 incubator. MDA-MB-231 cells were transfected with pIRES2-SHH-EGFP (gifted by Dr. Wade Bushman, University of Wisconsin, WI) and selected in medium supplemented with 500 μg/ml geneticin (Invitrogen). MCF10AT cells stably expressing SHH were generated by transfecting pIRES3-SHH-EGFP and selected in medium supplemented with 250 ng/ml Puromycin (Invitrogen). MDA-MB-231 cells stably silenced for CYR61 using shRNA cloned into pSUPER were selected in medium supplemented with 500 μg/ml Geneticin and 300 μg/ml Puromycin. All experiments were performed within no greater than 10 passages from each other in order to ensure genotypic and phenotypic fidelity between experiments.

Conditioned media (CM) was harvested from 1×10^6 cells after 18 hrs, cleared by centrifugation at 800 rpms for 8 minutes and used in assays described below.

Quantitative Real-Time Polymerase Chain Reaction (qRT-PCR)

cDNA was synthesized from total RNA (1μg) using the High Capacity Reverse Transcriptase Kit (Applied Biosystems, Foster City, CA) using the following conditions: 25°C for10 minutes, 37°C for 120 minutes, 85°C for 5 seconds. Expression of SHH and CYR61 was assessed using primer probes (Applied Bioystems) in the BioRad iQ5 Real-Time Detection System (Bio-Rad, Hercules, CA) using the Applied Biosystem 2-Step PCR program. GAPDH or β-actin served as endorse control genes. Amplified gene transcripts were normalized to the endorse control genes (CT_{gene}-CTcontrol= CT). The fold changes observed in the experimental groups were expressed as ratios of Experimental (2^- (ct))/ Control ($2^{-(}$ ct)). Each experiment was performed in triplicate and repeated at least once. SHH and CYR61 mRNA expression in human breast cancer patient tissues was analyzed using tissue qPCR array cDNA samples from OriGene Technologies (Rockville, MD). qPCR was performed per the manufacturers' recommendations. Fold changes in expression were calculated relative to endorse control, β-actin (Gulhati *et al.*, 2011; Trimmer *et al.*, 2010).

Western Blot Analysis

Lysates of cells were harvested in NP-40 buffer and quantitated spectrophotomically. Equal amounts of protein were and resolved by SDS-PAGE. Proteins were immunoblotted for SHH (N-19; Santa Cruz), Cyr61 (H-78; Santa Cruz), GAPDH (Cell Signaling, Beverly, MA), or α/β tubulin (Cell Signaling) Blots were developed using SuperSignal (Pierce, Rockford, IL) and imaged on a Fuji LAS3000 imager.

Mass spectrometry analysis

Secreted proteomes were isolated, and analyzed as described previously (Mbeunkui *et al.*, 2007). Details are as follows: Serum free media was added to a 100 mm tissue culture plate seeded with 8×10^5 cells. After 16 hours, the serum free, conditioned, media was acidified with 10% trifluoroacetic acid (TFA) to promote protein stabilization. Proteins were isolated and fractioned from media using a tC2 reverse phase column and eluted using increasing concentrations of acetonitrile. Eluted proteins we were dried and trypsin digested overnight in an ammonium bicarbonate/tris(2-carboxylethyl) phosphine (ABC/TCEP) solution at 37°C. An initial 2μl/min fraction was injected for MS/MS Q-TOF analysis to determine sample preparation's peptide concentration and quality. Final data was collected from a 180 minute analysis for each sample. Analysis of equal concentrations of peptide injections per experimental group were made using the Mascot, database software which provided a list of proteins, that matched the peptides amino acid signatures identified during the ms/ms analysis. Identified proteins were compared for each experimental group.

Wound Healing

A "scratch" was made in the cell monolayer with a sterile 20μm pipette tip. Images were recorded (three per well) at 10X magnification using Nikon Eclipse TE 2000-U (Nikon

Instruments Inc. Melville, NY). This was considered as T_0. Following incubation for 10 hours at 37°C, the wells were imaged again at the same 10 places where captured at T_0. The experiment was conducted in duplicate and cell motility was expressed as $(T_0-T_{10})/T_0$ which represents the rate of movement over 10 hours.

Transwell Migration

Cells suspended in serum-free media were added to gelatin (6 ng/ml)-coated sterile 8μm pore inserts. The lower chambers of the wells were filled with 10%FBS containing media and incubated at 37°C for 5 hours. The interior of the insert/filters were carefully cleaned and the filters stained with crystal violet. Eight random frames of each insert were photographed using Nikon Eclipse TE 2000-U and the stained cells in each frame were enumerated. Each experimental group was assayed in triplicate.

Transwell Invasion

Cell suspension in serum-free media was added into sterile 8 μm pore Matrigel®-coated filters (BD, Fraklin Lakes NJ). The inserts were lowered into 24-well plates containing 10 μg/ml fibronectin containing media and incubated at 37°C for 18 hours. Staining and result recording was performed in the same way as the migration assay described above.

Endothelial cell migration and invasion assays were done in the same manner as described above with a few changes. Primary rat lung derived microvascular endothelial cells (MVECS) (USA Center For Lung Biology Core, Mobile AL) were seeded into the upper chambers previously hydrated inserts and migration/invasion was recorded in response to conditioned media from each experimental group or recombinant SHH (R&D Systems, Minneapolis MN) or 100 ng/ml VEGF (R&D Systems). All experimental groups were assayed in triplicate.

Cell Proliferation

Cells were plated in triplicate in 24-well tissue culture plates. Each day cells were detached and counted using a hemocytometer. The assay duration was 7 days. Counting for each cell type was done for each day in triplicate.

Anchorage-independent growth (Soft Agar Colony Formation)

Cells (4000) from each experimental group were mixed in a 1:1 ratio with 0.7 % agar in DMEM/F12 supplemented with 10 % serum and layered on to a bed of 1.5 % agar in serum-free media. The agar was kept hydrated with fresh growth medium. The assay was terminated after 4 weeks and colonies with   50 cells were counted under a microscope. Colonies were also stained using 1:100 diluted crystal violet and recounted. Each experimental group was assayed in triplicate.

Foci Formation

Five hundred cells were disseminated in triplicate in 10mm cell culture plates. At the end of three weeks foci were fixed using methanol, stained using crystal violet and counted.

Endothelial Cell Network Formation

MVEC cell suspension in conditioned media from test groups was added to wells containing Growth Factor Reduced Matrigel® (BD). After 6 hrs network formations were counted using the Nikon Elements image analysis software. Network lengths were measured from branch-point to the next adjacent branch-point within the network structures (Arnaoutova and Kleinman, 2010).

Luciferase Assay

Cells were transfected with reporter and effector constructs as follows: Tumor cells were co-transfected with pLNCX or pLNCX-GLI and pGL3-8xGLI (gifted by Dr. Philip Beachy, Stanford University, CA; the 8X Gli fragment was sub-cloned into pGL3 promoter vector) or pGL3-CYR61 promoter to assess GLI binding, Hh signaling activation and CYR61 regulation respectively. 33-40hrs post-transfection cells were lysed overnight and assessed for luciferase activity. Data is normalized to total protein concentration. Each assay was done in triplicate and reproduced three times.

The GLI-binding site in the promoter of CYR61 was mutated (pGL3-GLI/M-CYR61) or deleted (pGL3-GLI/D-CYR61) b y inside-out PCR with the following primers: GLI/M-Forward: gcggccgccccacccag/Reverse: ctgagagggaggaacaaaag, GLI/D-Forward: ccacccagtccaggca/ Reverse: ctgagagggaggaacaaaag.

Chromatin Immunoprecipitation Assay (ChIP)

MDA-MB-231-pIRES2-EGFP (control) and MDA-MB-231-pIRES2-SHH were processed for immunoprecipitation using the ChIP-IT Express Enzymatic kit (Active Motif, Carlsbad, CA) according to the manufacturer's protocol and recommendations. GLI1(C-18; sc-6152x; Santa Cruz) and normal rabbit IgG were used for immunoprecipitation. Primers targeting the putative GLI1 binding region in the promoter of CYR61 (Forward: cggtcaactcgcatcacc and Reverse: cgacttatgttgggaaggg) amplified a 165 base pair product from sheared immunoprecipitated chromatin template. Non-targeting primers (Forward: gccctgcgaccacaccaa and Reverse: cgtatgcgctttcgttggg) were also used as a negative control for primer specificity. PCR products were visualized on a 2.5 % agarose gel.

Animal Experiments

Experiments were conducted under protocol approved by the Institutional Animal Care and Use Committee (IACUC) of the University of South Alabama, Mobile. Cells (200,000) were injected into the mammary fat pad of female six week old athymic nude mice, as previously described (Das *et al.*, 2009; Shevde *et al.*, 2006). Mice were monitored biweekly for tumor development. Tumors were excised via survival surgery when they attained a mean tumor diameter of 10 mm. Ten weeks post tumor excision mice were euthanized and assessed for pulmonary metastasis. Pulmonary metastases were assessed by 1) GFP-expressing tumor cells in the lungs detected under UV-FITC, 2) staining with Bouin's reagent and 3) recovery of GFP-expressing tumor cells from the lungs in cell culture.

Isolation of Metastatic Breast Cancer Cells from Mice Lungs—Lungs harvested from mice were homogenized to recover a cell suspension that was re-suspended in fresh

cell culture media supplemented with appropriate selection antibiotics. Cells were incubated and grown according to cell culture methods described above.

Immunohistochemistry

Xenografted mice tissues were fixed in 10% formalin and embedded into paraffin. Sections (4 μm) were processed for immunohistochemistry. Excised tumor tissues were examined for SHH, Ki67 (cell proliferation), Griffonia (Bandeiraea) Simplicifolia Lectin I isolectin B4 (Vector Laboratories, Burlingame, CA) (endothelial cell surface marker/angiogenesis) (Singh *et al.*, 2009) and CYR61 diluted in Antibody Diluent from BD Pharmingen. Deparaffinized sections were subject to antigen retrieval in citrate buffer (Antigen Unmasking Solution, Vector Laboratories) in a decloaking chamber (Biocare Medical, Concord, CA) at 125°C for 30 seconds. Tissue sections were probed with primary antibodies: anti-SHH (1:50 Millipore, Temecula, CA), anti-Lectin (1:25, Vector Laboratories, Inc., Burlingame CA), anti-CYR61 (1:300, Santa Cruz CA) followed by appropriate secondary antibodies and using the DAB peroxidase solution (VECTOR Laboratories). The staining intensity was represented as an immunoreactive score (Metge *et al.*, 2008). Microvessel density was quantitated directly by counting the number of positive vessels that were stained.

Statistical Analysis

Statistical analyses between experimental groups were assessed using GraphPad Prism 4 (San Diego, CA). Student's t-test, Mann-Whitney, one-way ANOVA, or two-way ANOVA were applied based on the statistical mandates or suggestions of each analysis.

Supplementary Material

Refer to Web version on PubMed Central for supplementary material.

ACKNOWLEDGMENTS

ABBREVIATIONS

CYR61	Cysteine-rich angiogenic inducer, 61
Hh	Hedgehog pathway
MVD	Microvessel Density
SHH	Sonic Hedgehog ligand

References

Arnaoutova I, Kleinman HK. In vitro angiogenesis: endothelial cell tube formation on gelled basement membrane extract. Nat Protoc. 2010; 5:628–35. [PubMed: 20224563]

Babic AM, Kireeva ML, Kolesnikova TV, Lau LF. CYR61, a product of a growth factor-inducible immediate early gene, promotes angiogenesis and tumor growth. Proc Natl Acad Sci U S A. 1998; 95:6355–60. [PubMed: 9600969]

Bailey JM, Mohr AM, Hollingsworth MA. Sonic hedgehog paracrine signaling regulates metastasis and lymphangiogenesis in pancreatic cancer. Oncogene. 2009; 28:3513–25. [PubMed: 19633682]

Beachy PA, Hymowitz SG, Lazarus RA, Leahy DJ, Siebold C. Interactions between Hedgehog proteins and their binding partners come into view. Genes Dev. 2010; 24:2001–12. [PubMed: 20844013]

Bicknell R, Harris AL. Novel angiogenic signaling pathways and vascular targets. Annu Rev Pharmacol Toxicol. 2004; 44:219–38. [PubMed: 14744245]

Blagosklonny MV. Antiangiogenic therapy and tumor progression. Cancer Cell. 2004; 5:13–7. [PubMed: 14749122]

Byrd N, Grabel L. Hedgehog signaling in murine vasculogenesis and angiogenesis. Trends Cardiovasc Med. 2004; 14:308–13. [PubMed: 15596107]

Cao X, Geradts J, Dewhirst MW, Lo HW. Upregulation of VEGF-A and CD24 gene expression by the tGLI1 transcription factor contributes to the aggressive behavior of breast cancer cells. Oncogene. 2011:1–12. doi: 10.1038/onc.2011.219.

Chen C-C, Lau LF. Functions and mechanisms of action of CCN matricellular proteins. The International Journal of Biochemistry & Cell Biology. 2009; 41:771–783. [PubMed: 18775791]

Chen CC, Mo FE, Lau LF. The angiogenic factor Cyr61 activates a genetic program for wound healing in human skin fibroblasts. J Biol Chem. 2001; 276:47329–37. [PubMed: 11584015]

Chinchilla P, Xiao L, Kazanietz MG, Riobo NA. Hedgehog proteins activate pro-angiogenic responses in endothelial cells through non-canonical signaling pathways. Cell Cycle. 2010; 9:570–79. [PubMed: 20081366]

Cohen MM Jr. Hedgehog signaling update. Am J Med Genet A. 2010; 152A:1875–914. [PubMed: 20635334]

Das S, Harris LG, Metge BJ, Liu S, Riker AI, Samant RS, et al. The hedgehog pathway transcription factor GLI1 promotes malignant behavior of cancer cells by up-regulating osteopontin. The Journal of Biological Chemistry. 2009; 284:22888–22897. [PubMed: 19556240]

Das S, Samant RS, Shevde LA. Hedgehog signaling induced by breast cancer cells promotes osteoclastogenesis and osteolysis. J Biol Chem. 2011; 286:9612–22. [PubMed: 21169638]

Dobroff AS, Wang H, Melnikova VO, Villares GJ, Zigler M, Huang L, et al. Silencing cAMP-response element-binding protein (CREB) identifies CYR61 as a tumor suppressor gene in melanoma. J Biol Chem. 2009; 284:26194–206. [PubMed: 19632997]

Feng P, Wang B, Ren EC. Cyr61/CCN1 is a tumor suppressor in human hepatocellular carcinoma and involved in DNA damage response. Int J Biochem Cell Biol. 2008; 40:98–109. [PubMed: 17698398]

Fox SB, Generali DG, Harris AL. Breast tumour angiogenesis. Breast Cancer Research: BCR. 2007; 9:216–216. [PubMed: 18190723]

Gulhati P, Bowen KA, Liu J, Stevens PD, Rychahou PG, Chen M, et al. mTORC1 and mTORC2 regulate EMT, motility, and metastasis of colorectal cancer via RhoA and Rac1 signaling pathways. Cancer Res. 2011; 71:3246–56. [PubMed: 21430067]

Hochman E, Castiel A, Jacob-Hirsch J, Amariglio N, Izraeli S. Molecular pathways regulating pro-migratory effects of Hedgehog signaling. J Biol Chem. 2006; 281:33860–70. [PubMed: 16943197]

Kanda S, Mochizuki Y, Suematsu T, Miyata Y, Nomata K, Kanetake H. Sonic hedgehog induces capillary morphogenesis by endothelial cells through phosphoinositide 3-kinase. J Biol Chem. 2003; 278:8244–9. [PubMed: 12514186]

Kleer CG, Zhang Y, Merajver SD. CCN6 (WISP3) as a new regulator of the epithelial phenotype in breast cancer. Cells Tissues Organs. 2007; 185:95–9. [PubMed: 17587813]

Lai D, Ho KC, Hao Y, Yang X. Taxol resistance in breast cancer cells is mediated by the hippo pathway component TAZ and its downstream transcriptional targets Cyr61 and CTGF. Cancer Res. 2011; 71:2728–38. [PubMed: 21349946]

Leu SJ, Lam SC, Lau LF. Pro-angiogenic activities of CYR61 (CCN1) mediated through integrins alphavbeta3 and alpha6beta1 in human umbilical vein endothelial cells. J Biol Chem. 2002; 277:46248–55. [PubMed: 12364323]

Lin MT, Zuon CY, Chang CC, Chen ST, Chen CP, Lin BR, et al. Cyr61 induces gastric cancer cell motility/invasion via activation of the integrin/nuclear factor-kappaB/cyclooxygenase-2 signaling pathway. Clin Cancer Res. 2005; 11:5809–20. [PubMed: 16115920]

Lu ZH, Jia J, Ren J, Ma B, Di LJ, Song GH. Detection of breast cancer stem cells and the expression of key molecules in Hedgehog signaling pathway. Beijing Da Xue Xue Bao. 2008; 40:480–5. [PubMed: 18931709]

Mancuso MR, Davis R, Norberg SM, O'Brien S, Sennino B, Nakahara T, et al. Rapid vascular regrowth in tumors after reversal of VEGF inhibition. J Clin Invest. 2006; 116:2610–21. [PubMed: 17016557]

Mazumdar T, Devecchio J, Agyeman A, Shi T, Houghton JA. The GLI genes as the molecular switch in disrupting Hedgehog signaling in colon cancer. Oncotarget. Aug 17.2011 2011. Epub ahead of print.

Mbeunkui F, Metge BJ, Shevde LA, Pannell LK. Identification of differentially secreted biomarkers using LC-MS/MS in isogenic cell lines representing a progression of breast cancer. J Proteome Res. 2007; 6:2993–3002. [PubMed: 17608509]

Merchant AA, Matsui W. Targeting Hedgehog--a cancer stem cell pathway. Clin Cancer Res. 2010; 16:3130–40. [PubMed: 20530699]

Metge BJ, Frost AR, King JA, Dyess DL, Welch DR, Samant RS, et al. Epigenetic silencing contributes to the loss of BRMS1 expression in breast cancer. Clin Exp Metastasis. 2008; 25:753–63. [PubMed: 18566899]

Mukherjee S, Frolova N, Sadlonova A, Novak Z, Steg A, Page GP, et al. Hedgehog signaling and response to cyclopamine differ in epithelial and stromal cells in benign breast and breast cancer. Cancer Biol Ther. 2006; 5:674–83. [PubMed: 16855373]

O'Toole SA, Machalek DA, Shearer RF, Millar EK, Nair R, Schofield P, et al. Hedgehog Overexpression Is Associated with Stromal Interactions and Predicts for Poor Outcome in Breast Cancer. Cancer Res. 2011; 71:4002–4014. [PubMed: 21632555]

Pola R, Ling LE, Silver M, Corbley MJ, Kearney M, Blake Pepinsky R, et al. The morphogen Sonic hedgehog is an indirect angiogenic agent upregulating two families of angiogenic growth factors. Nat Med. 2001; 7:706–11. [PubMed: 11385508]

Porter JA, von Kessler DP, Ekker SC, Young KE, Lee JJ, Moses K, et al. The product of hedgehog autoproteolytic cleavage active in local and long-range signalling. Nature. 1995; 374:363–6. [PubMed: 7885476]

Renault MA, Roncalli J, Tongers J, Thorne T, Klyachko E, Misener S, et al. Sonic hedgehog induces angiogenesis via Rho kinase-dependent signaling in endothelial cells. J Mol Cell Cardiol. 2010; 49:490–8. [PubMed: 20478312]

Samant RS, Shevde LA. Recent advances in anti-angiogenic therapy of cancer. Oncotarget. 2011; 2:122–34. [PubMed: 21399234]

Santner SJ, Dawson PJ, Tait L, Soule HD, Eliason J, Mohamed AN, et al. Malignant MCF10CA1 cell lines derived from premalignant human breast epithelial MCF10AT cells. Breast Cancer Res Treat. 2001; 65:101–10. [PubMed: 11261825]

Shevde LA, Samant RS, Paik JC, Metge BJ, Chambers AF, Casey G, et al. Osteopontin knockdown suppresses tumorigenicity of human metastatic breast carcinoma, MDA-MB-435. Clinical & Experimental Metastasis. 2006; 23:123–133. [PubMed: 16830223]

Singh S, Varney M, Singh RK. Host CXCR2-dependent regulation of melanoma growth, angiogenesis, and experimental lung metastasis. Cancer Res. 2009; 69:411–5. [PubMed: 19147552]

Sun ZJ, Wang Y, Cai Z, Chen PP, Tong XJ, Xie D. Involvement of Cyr61 in growth, migration, and metastasis of prostate cancer cells. Br J Cancer. 2008; 99:1656–67. [PubMed: 18941464]

Trimmer C, Whitaker-Menezes D, Bonuccelli G, Milliman JN, Daumer KM, Aplin AE, et al. CAV1 inhibits metastatic potential in melanomas through suppression of the integrin/Src/FAK signaling pathway. Cancer Res. 2010; 70:7489–99. [PubMed: 20709760]

Tsai MS, Bogart DF, Castaneda JM, Li P, Lupu R. Cyr61 promotes breast tumorigenesis and cancer progression. Oncogene. 2002; 21:8178–85. [PubMed: 12444554]

Vokes SA, Yatskievych TA, Heimark RL, McMahon J, McMahon AP, Antin PB, et al. Hedgehog signaling is essential for endothelial tube formation during vasculogenesis. Development. 2004; 131:4371–80. [PubMed: 15294868]

Weidner N, Semple JP, Welch WR, Folkman J. Tumor angiogenesis and metastasis--correlation in invasive breast carcinoma. N Engl J Med. 1991; 324:1–8. [PubMed: 1701519]

Xie D, Miller CW, O'Kelly J, Nakachi K, Sakashita A, Said JW, et al. Breast cancer. Cyr61 is overexpressed, estrogen-inducible, and associated with more advanced disease. J Biol Chem. 2001a; 276:14187–94. [PubMed: 11297518]

Xie D, Nakachi K, Wang H, Elashoff R, Koeffler HP. Elevated levels of connective tissue growth factor, WISP-1, and CYR61 in primary breast cancers associated with more advanced features. Cancer Res. 2001b; 61:8917–23. [PubMed: 11751417]

Xie D, Yin D, Wang HJ, Liu GT, Elashoff R, Black K, et al. Levels of expression of CYR61 and CTGF are prognostic for tumor progression and survival of individuals with gliomas. Clin Cancer Res. 2004; 10:2072–81. [PubMed: 15041728]

Yang L, Xie G, Fan Q, Xie J. Activation of the hedgehog-signaling pathway in human cancer and the clinical implications. Oncogene. 2010; 29:469–81. [PubMed: 19935712]

Zetter BR. Angiogenesis and tumor metastasis. Annu Rev Med. 1998; 49:407–24. [PubMed: 9509272]

Zhang RD, Fidler IJ, Price JE. Relative malignant potential of human breast carcinoma cell lines established from pleural effusions and a brain metastasis. Invasion Metastasis. 1991; 11:204–15. [PubMed: 1765433]

Zhou ZQ, Cao WH, Xie JJ, Lin J, Shen ZY, Zhang QY, et al. Expression and prognostic significance of THBS1, Cyr61 and CTGF in esophageal squamous cell carcinoma. BMC Cancer. 2009; 9:291. [PubMed: 19698122]

Zunich SM, Douglas T, Valdovinos M, Chang T, Bushman W, Walterhouse D, et al. Paracrine sonic hedgehog signalling by prostate cancer cells induces osteoblast differentiation. Mol Cancer. 2009; 8:12. [PubMed: 19254376]
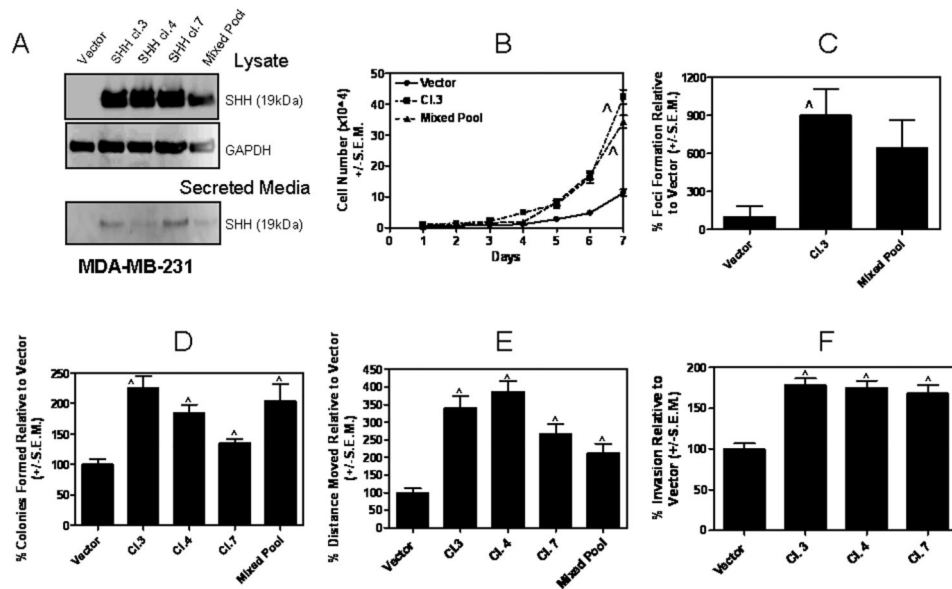
Figure 1. Constitutive Hh signaling in breast cancer cell lines enhances their malignant attributes

A) Cell lysates and concentrated (10X) conditioned media from each experimental group for stable SHH-expressors of MDA-MB-231 cells were assessed by western blot analyses. Activated Hh signaling significantly enhances **B)** Cell proliferation (^p < 0.001, for both, SHH cl. 3 and Mixed Pool relative to Vector control cells), **C)** Contact independent growth (^p = 0.03 for SHH cl. 3, and p > 0.05 for Mixed Pool relative to vector controls), **D)** Anchorage independent growth (^p < 0.0001 for all SHH-expressing groups relative to vector control cells), **E)** Non-chemotactic cell movement (^p < 0.0001 for all SHH-expressing groups relative to vector control cells) and, **F)** Invasion through Matrigel (^p < 0.0001 for all SHH-expressing groups relative to vector control cells).
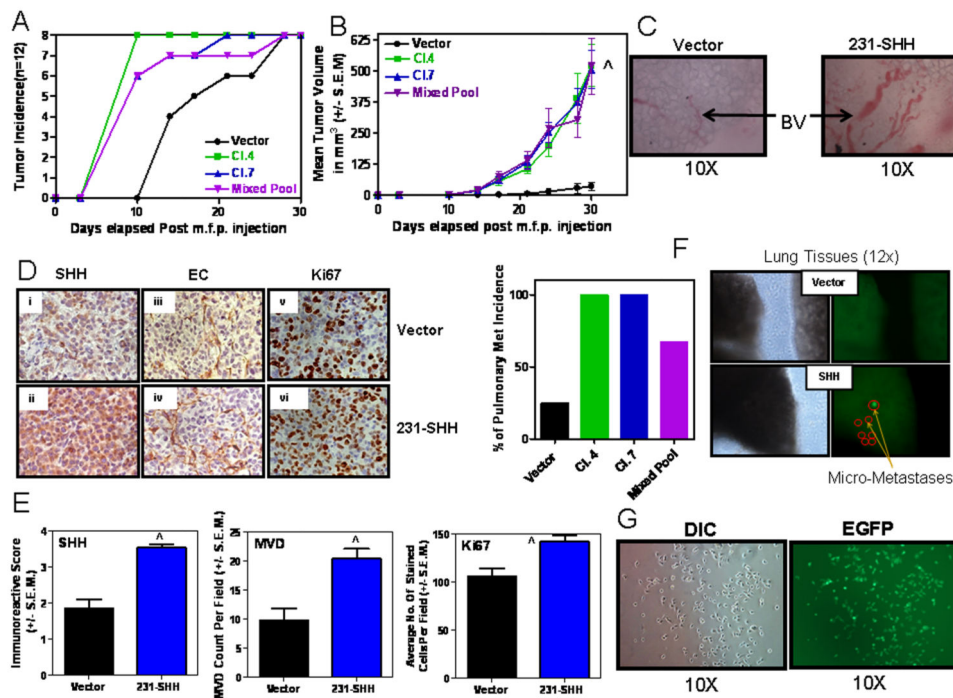
Figure 2. Constitutive SHH expression in MDA-MB-231 cells potentiates tumor growth and spontaneous metastasis

200,000 cells were injected into the mammary fat pad of athymic nude mice. **A)** All mice injected with SHH-expressing breast cancer cell lines developed palpable tumors 10 days after injection. However, mice in the cohort of the vector control cells lagged behind. **B)** SHH expressing mice showed significantly increased tumor growth (^p < 0.0001 for all SHH-expressing groups relative to vector) and, **C)** prominently increased blood vessel (BV) formation in the primary tumors. **D)** The xenografts obtained from the MDA-MB-231-SHH expressing cells show a greater staining intensity for SHH (Panels i and ii), endothelial cells staining for lectin (Panels iii and iv) and Ki67 (Panels v and vi). **E)** Concomitant with staining intensity, the xenografts obtained from MDA-MB-231-SHH cells show greater immunoreactive scores for SHH (^p < 0.0001), microvessel density, MVD (^p = 0.0019) and Ki67 (^p = 0.0062). **F)** Tumors from SHH expressing cells also yielded a high incidence of pulmonary metastasis. Shown are representative photomicrographs of the lung images using the Stereoscopic Zoom Microscope (Nikon SMZ1500, Nikon Instruments Inc. Melville, NY) denoting visible light (left panels) and u.v. fluorescence (right panels) imaging that allows visualization of EGFP-expressing metastatic cells. **G)** The EGFP-expressing metastatic cells from the lungs were isolated in culture. Shown are representative photomicrographs in DIC and u.v. fluorescence.
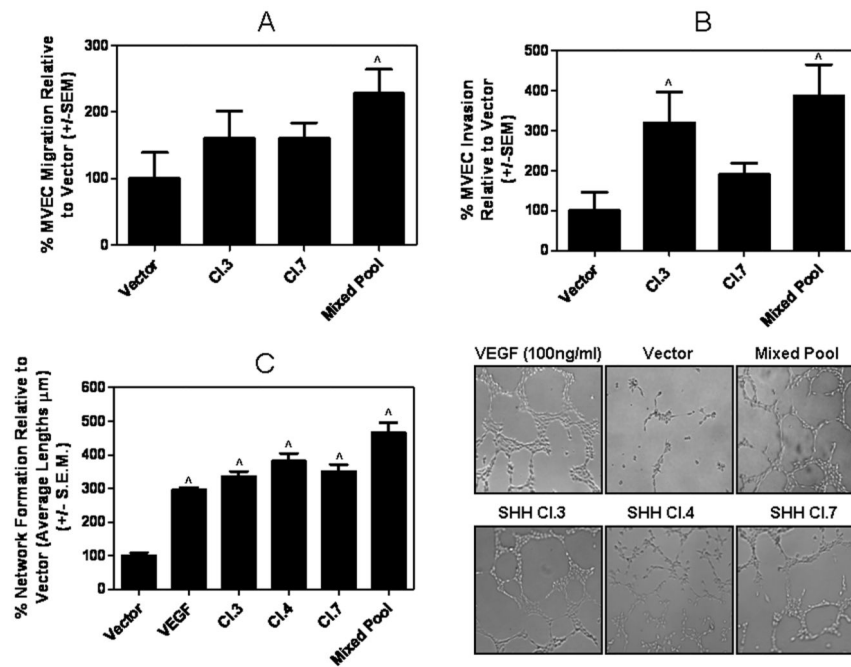
Figure 3. Factors secreted by breast cancer cell with constitutive Hh signaling promote pro-angiogenic behavior of endothelial cells *in vitro*

Conditioned media from SHH expressing cell lines enhances microvascular endothelial cell **A)** migration (^p = 0.003), **B)** invasion (^p < 0.02 for SHH Cl. 3 and Mixed Pool relative to vector) and **C)** promotes endothelial cell network formation (^p < 0.0001 for all SHH-expressing groups relative to vector control cells), which is critical for lumen formation *in vivo*. SHH expression promotes the formation of networks that are comparable if not exceeding that of VEGF (positive control).
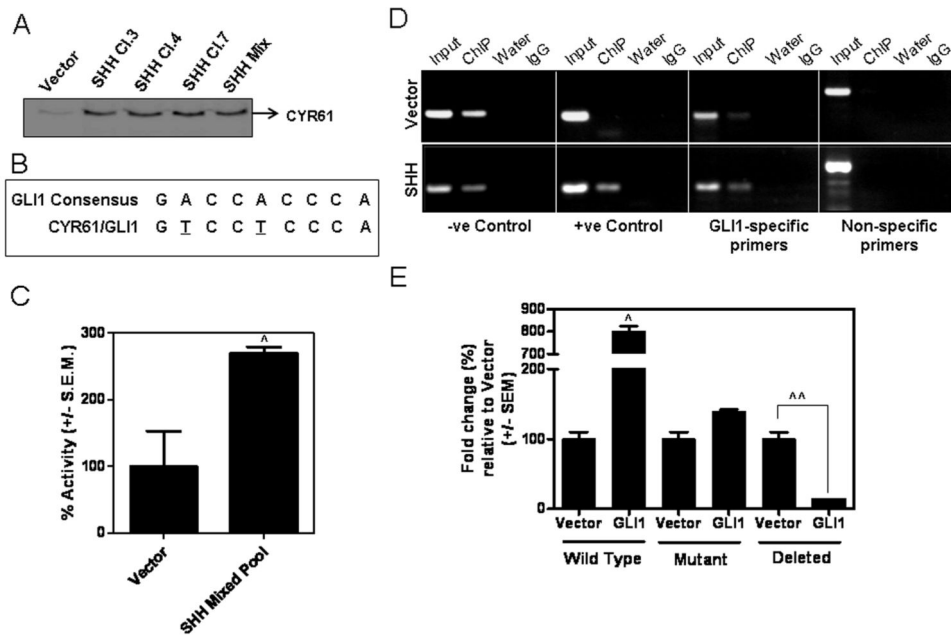
Figure 4. GLI1 transcriptionally targets CYR61 gene expression
A) CYR61 is notably more abundant in SHH expressing cell secretome compared to vector. Equal numbers of cells from each experimental group were seeded and allowed to attach overnight. The following day cells were washed and cultured in SFM. 18 hrs later, conditioned media was harvested and equal amounts of media were analyzed via western blot for the expression of CYR61. Immuno detection confirmed what was seen in the proteomics analysis. **B)** Analysis of approximately 1 kB upstream of the transcriptional start site determined that the CYR61 promoter region contains a putative GLI1-recognition sequence that differs from the consensus GLI1-binding region by two nucleotides (underscored) sequence. **C)** The CYR61 promoter is activated (^p < 0.0001) in breast cancer cell lines expressing SHH. Reporter assays were done using a luciferase-expressing CYR61 promoter in vector-control and SHH-expressing MDA-MB-231 cells. **D)** ChIP assay confirms that GLI1 binds to the promoter of CYR61. Input: Total native chromatin isolated from cancer cells (indicated, vector-transfected or SHH-expressing); ChIP: PCR amplified DNA product is generated after immunoprecipitation with GLI1 antibody; Water: PCR water-control used to assess quality and lack of contamination; IgG: Isotype control; −ve and +ve control denote kit-provided negative and positive control primers respectively; GLI1-specific primers were used to amplify the putative GLI1 binding site in CYR61 promoter region, and non-specific primers were used as a control to amplify a region 1KB downstream of the putative GLI1 binding in CYR61 promoter that is void of the GLI1 consensus sequence. **E)** COS7 cells were transfected with CYR61 promoter and empty vector or GLI1-expressing construct. While the wild-type CYR61 promoter bearing the GLI-binding site is significantly upregulated (8-fold; ^p < 0.0001), mutation or deletion of the GLI binding site in the CYR61 promoter results in abrogation (^^p < 0.005) of luciferase reporter activity of the CYR61 promoter indicating that GLI1 transcriptionally regulates CYR61 gene expression.
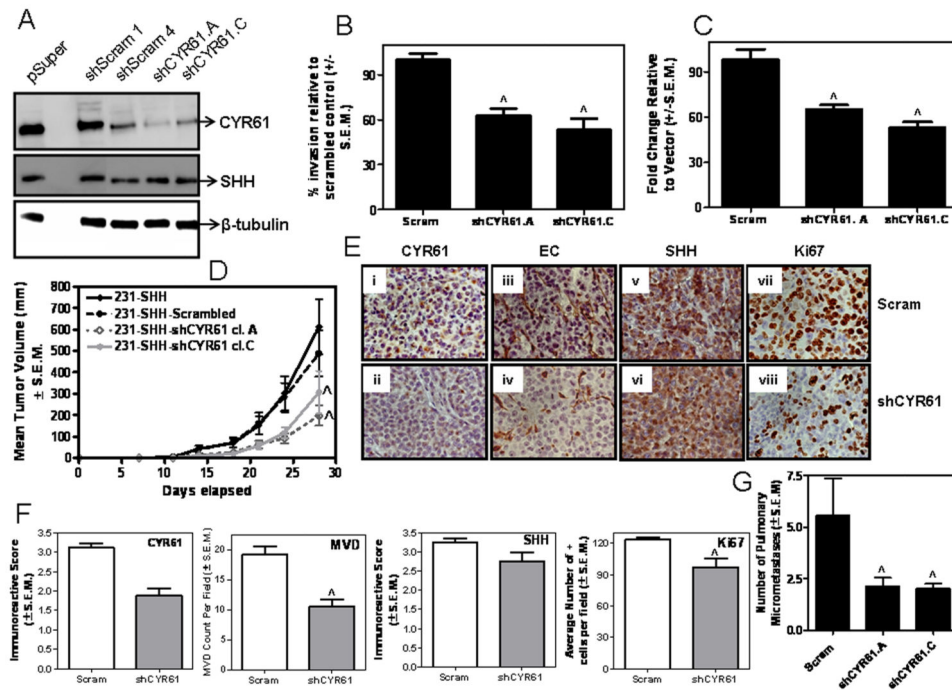
Figure 5. Abrogating CYR61 expression in SHH-expressing cells mitigates the effects of constitutive Hh signaling in MDA-MB-231 cells

A) Stable silencing of endogenous CYR61 expression using shRNA results in **B)** decreased invasive behavior (^p < 0.0001 relative to Scrambled shRNA control (Scram)), **C)** reduced ability to induce endothelial cell network formation (^p < 0.0001 relative to control (Scram)) and, **D)** significantly slower (^p = 0.01) tumor xenograft growth in female, athymic nude mice relative to scrambled shRNA transfected cells (MDA-MB-231-SHH-Scram). **E)** Immunohistochemical analysis of the primary tumor xenograft tissue for CYR61 (Panels i and ii), angiogenic microvessels (Panels iii and iv), SHH (Panels v and vi) (p > 0.05) and Ki67 (Panels vii and viii). Shown are representative images for control (Scram) and MDA-MB-231-SHH cells stably transfected with shRNA to CYR61. **F)** The xenografts obtained from MDA-MB-231-SHH-shCYR61 cells show lower immunoreactive scores for CYR61, microvessel density, MVD (^p = 0.0006) and Ki67 (^p = 0.0062). The levels of SHH expression were comparable between the control (Scram) and cells silenced stably for CYR61. **G)** The incidence of spontaneous pulmonary metastasis is decreased in CYR61-silenced SHH-expressing MDA-MB-231 cells (^p =0.01).
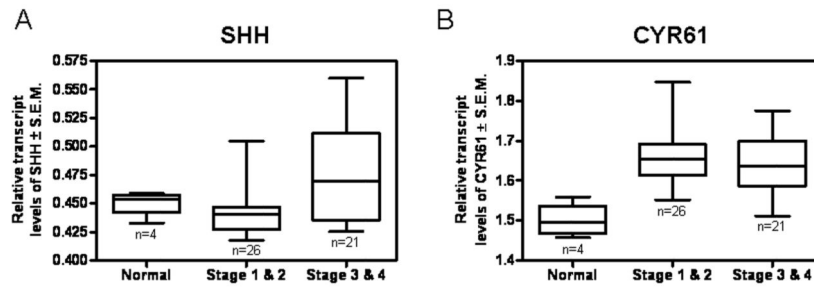
Figure 6. The expression of SHH and CYR61 are increased in advanced breast tumors
We assessed the transcript levels of SHH and CYR61 in a panel of tissues encompassing normal breast tissue (n=4) and breast tumor tissues by QRT-PCR. The panel included tissues representing Stage 1 (n=2), Stage 2 (n=24) and Stage 3 & 4 (n=21). **A)** Overall, the transcript levels of SHH are elevated in breast tumors derived from advanced stage breast cancer ($^\wedge$p = 0.0027). **B)** The transcript levels of CYR61 are significantly higher in advanced stage breast cancer relative to normal tissues ($^\wedge$p = 0.0011). The data is represented as relative transcript levels of SHH and CYR61 normalized to β-actin.